Supporting Information for

Challenges and Opportunities for Machine Learning Potentials in Transition Path Sampling: Alanine Dipeptide and Azobenzene Studies

Nikita Fedik[1,2], Wei Li[3*], Nicholas Lubbers[3], Benjamin Nebgen[1], Sergei Tretiak[1,2,4], Ying Wai Li[3]

GitHub repository: https://github.com/nikitafedik/ml_tps_si

Data repository: https://zenodo.org/records/15047941

Molecular Dynamics Simulations

Thermal molecular dynamics (MD) simulations were performed using the Atomic Simulation Environment (ASE)[1] package with the HIP-NN-TS[2] model, trained on the ANI-1x dataset[3], as the calculator. Two systems — alanine dipeptide (AD) and azobenzene (AZ) — were studied to evaluate the accuracy of machine learning interatomic potentials (MLIPs).

For AD, four independent MD runs were initiated from four known isomers - C5, $C7_{ax}$, α_R and α_L - sourced from extensive theoretical study.[4] Each simulation was conducted with a timestep of 2 fs for 200,000 steps at 300 K, resulting in trajectories of 400 ps each. Combined, these runs yielded a total trajectory length of 1600 ps. As the MD simulations were run near room temperature, neighboring snapshots showed minimal differences. To reduce redundancy, every 80th step was selected, resulting in a final set of 10,000 random snapshots that broadly sampled the potential energy surface (PES). The Ramachandran plot depicting this sampling is shown in Fig S1A.

For AZ, two MD simulations were conducted for the cis and trans isomers using identical conditions: T = 300 K, timestep = 2 fs, friction coefficient = 0.1/fs, and 500,000 steps per simulation. Each trajectory spanned 1000 ps, amounting to a total trajectory length of 2000 ps across both runs. Every 100th step was retained to create a test set of 10,000 snapshots. Despite these long trajectories, most configurations remained clustered around cis- and trans- isomers, as AZ has high thermal activation barriers for isomerization (Fig S1B).

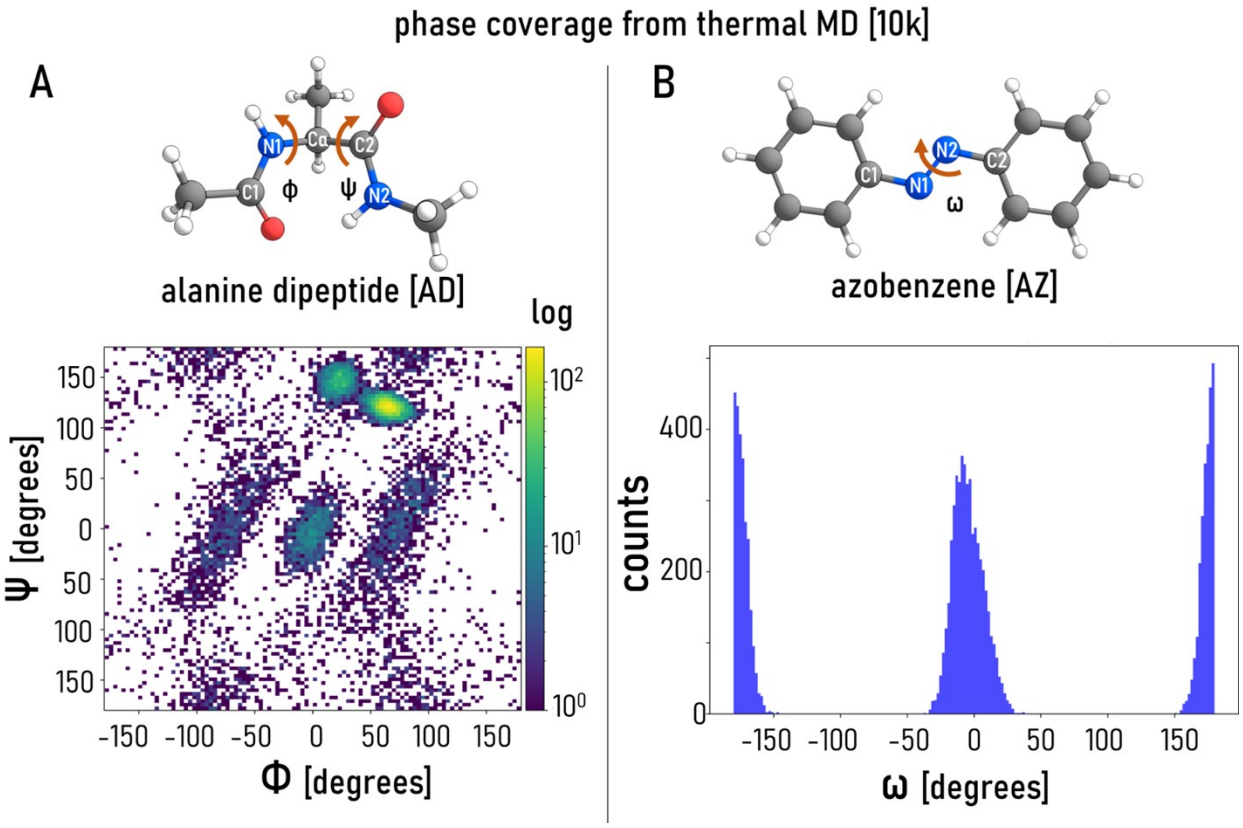

Figure S1. A. Alanine dipeptide (AD) structure and relevant dihedral angles ϕ and ψ. Ramachandran plot is based on the 10k configurations sampled from thermal MD trajectories of 1600ps. **B**. Azobenzene (AZ) structure with relevant dihedral angle ω highlighted. Histogramm depicts the frequency of visiting different ω values. As expected, thermal MD cannot sample rotational isomerization mechanism at 300K even at 2000ps combined trajectory.

Recalculation 10K MD Snapshots Using Various Methods

The selected snapshots for AD and AZ were recalculated using four methods:

1. Vanilla ANI-1x potential implemented in TorchANI[5].
2. Density Functional Theory (DFT) at the ωB97X/6-31G(d) level.
3. Sage2.0.2 potential from OpenFF[6,7].
4. Amber14 force field[8] through General Amber Force Field (GAFF)[9]

HIP-NN-TS outperformed all other methods in predicting energies and atomic forces compared to DFT references (Figure 1 and Figure S2).

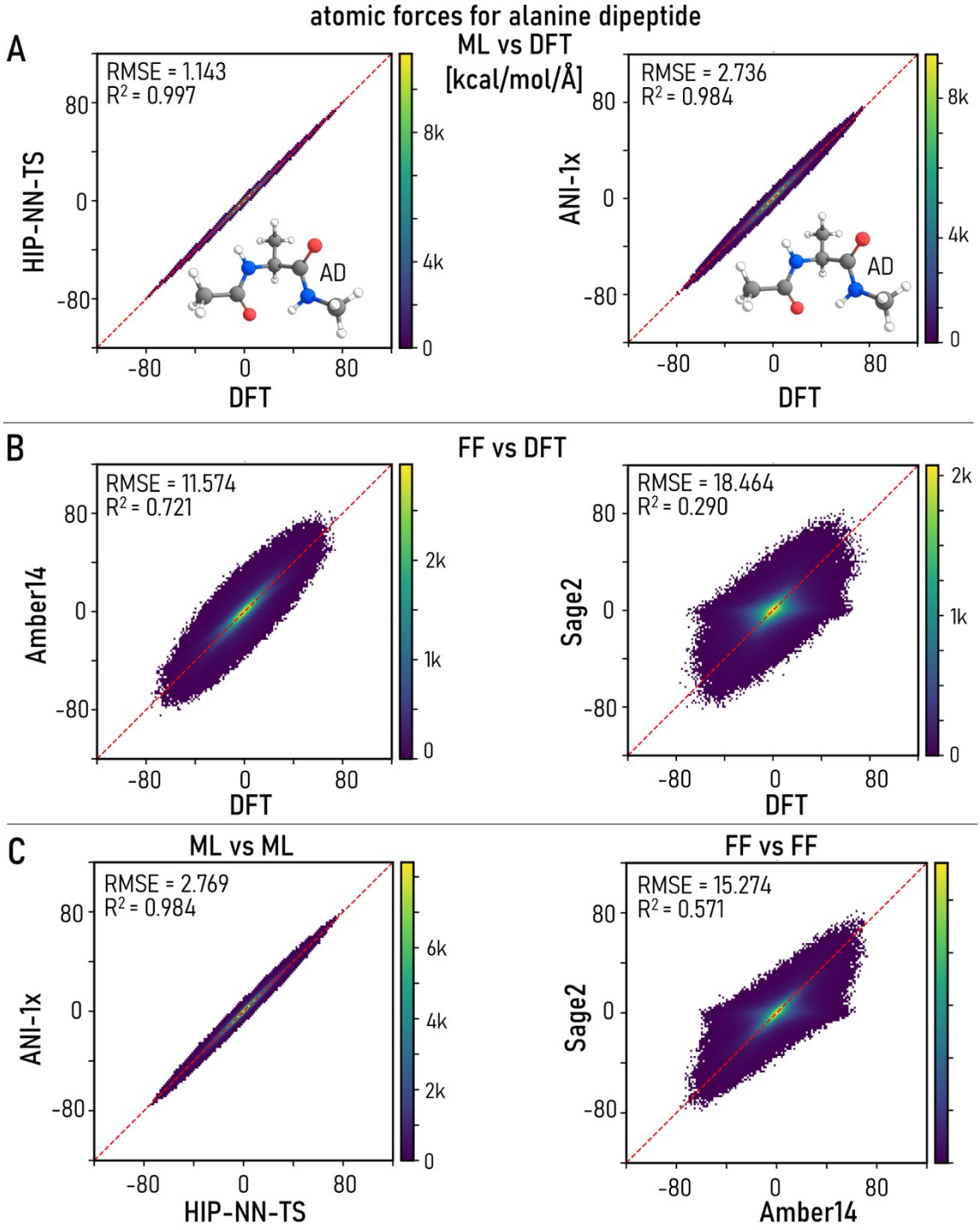

Figure S2. Evaluation of atomic forces (kcal/mol/Å) of 10k conformers taken from thermal MD trajectories for alanine dipeptide at 300K (see Fig S1 for chemical space coverage). Density correlation plots for atomic forces predictions by various models (MLIPs and FFs) against each other. **A**. MLIPs vs reference DFT. **B**. FFs vs DFT. **C**. MLIPs and FFs against each other. HIP-NN-TS demonstrates better correlation for atomic forces predictions than ANI-1x in line with the lower RMSE and MAE for both energies and forces (Table 2).

DFT Calculations

All DFT calculations for MD snapshots for both AD and AZ were performed using Gaussian09[10]at the ωB97X/6-31G(d)[11,12] level with tight SCF convergence criteria to align with the ANI-1x dataset. For AZ:

- The closed-shell DFT trajectory was computed by manually optimizing the transition state (TS) using the Berny algorithm (opt=TS) with suppressed curvature tests (calcfc, noeigentest). A smooth reaction coordinate near the TS was constructed via internal reaction coordinate (IRC) integration without recorrection steps. Default settings included a step size of 0.1 Bohr and recomputation of the Hessian every ten steps for a total trajectory length of up to 300 steps.
- The left and right shoulders of the trajectory—descents to cis and trans isomers—were determined by further optimizing final IRC states with Hessian calculations at each step for smoothness.
- Open-shell trajectories were built following a similar protocol but employed unrestricted broken-symmetry DFT with a default orbital shift (VShift) of 0.1 mHartree and HOMO-LUMO mixing. Wavefunction analysis confirmed TS instability (stable=opt).
- The expectation value of the spin-squared operator $\langle S^2 \rangle$ was analyzed along the open-shell rotational trajectory. Near the cis and trans isomers, $\langle S^2 \rangle$ values were close to zero, consistent with a closed-shell singlet ground state. However, at the TS, $\langle S^2 \rangle$ increased to 1.0, indicating significant spin contamination and an open-shell singlet character due to the biradical nature of the system. This behavior aligns with the expected electronic structure changes during azobenzene isomerization via the rotational pathway.

Classical Force Fields

Amber14

Many classical force fields (FFs) are primarily parameterized to work with biomolecules and are designed to map arbitrary molecules to known residues. To overcome this limitation and apply the Amber14 force field to alanine dipeptide (AD) and azobenzene (AZ), we used the Generalized Amber Force Field (GAFF) as implemented in the OpenMM[13] and OpenFF packages.

Single-point energies for each molecule were computed using the OpenMM package with the Amber14-all force field. The workflow began by reading an OpenFF Molecule object from an SDF file, after which partial charges were assigned using the MMFF94 charge scheme. To prepare the system, a SMIRNOFF template generator was employed to map the molecule's topology into the Amber14 parameterization. This setup enabled the calculation of single-point energies and atomic forces for 10,000 snapshots of isolated molecules generated during MD simulations.

For the rotational trajectory of AZ isomerization, this approach encountered challenges due to the presence of radicals near transition states. GAFF, as implemented in OpenFF/OpenMM, requires explicit connectivity and does not permit radicals. To address this limitation, we used SDF files generated

on-the-fly by OpenBabel for each configuration and set the bond order of the N=N bridge to 2 using the OpenBabel API along the entire trajectory. This adjustment ensured that bond connectivity remained consistent, even when the π-component of the N=N bond was broken.

Sage 2

The OpenFF initiative provides force fields explicitly crafted for small molecules, such as Sage2.0.2, which uses a SMIRNOFF template generator to map molecular coordinates and connectivity to known SMIRKS patterns[14]. We employed the latest Sage2.0.2 force field to calculate energies and atomic forces for 10,000 snapshots generated during MD simulations of AD and AZ, as well as for AZ isomerization processes. The procedure for applying Sage2.0.2 followed the same steps outlined above for Amber14.

Timings for energy + atomic forces evaluations

	device	evaluations/s	parameters
HIP-NN-TS	**GPU**	1316	batch size = 512
HIP-NN-TS	CPU	139	batch size = 2048
ANI-1x	**GPU**	2221	batch size = 10000
ANI-1x	CPU	746	batch size = 10000
Sage	CPU	64	48 threads
Amber	CPU	47	48 threads

Table S1. Timings for energy+atomic forces evaluations of employed methods. GPU computations have a green background. Amber14 and Sage 2.0.2 calculations in OpenMM/OpenFF were parallelized using a Python multiprocessing module with 48 threads. All calculations were performed on a single computational node with following specifications: 128 GB RAM, 2x16 cores AMD Rome Epyc 7282 CPU (2.8 Ghz) and Nvidia RTX A6000 GPU with 48 GB VRAM. Per user agreement, timings are not provided in the table but could be checked in DFT logs uploaded to Zenodo.

References:

1 A. H. Larsen, J. J. Mortensen, J. Blomqvist, I. E. Castelli, R. Christensen, M. Du\lak, J. Friis, M. N. Groves, B. Hammer, C. Hargus, E. D. Hermes, P. C. Jennings, P. B. Jensen, J. Kermode, J. R. Kitchin, E. L. Kolsbjerg, J. Kubal, K. Kaasbjerg, S. Lysgaard, J. B. Maronsson, T. Maxson, T. Olsen, L. Pastewka, A. Peterson, C. Rostgaard, J. Schiøtz, O. Schütt, M. Strange, K. S. Thygesen, T. Vegge, L. Vilhelmsen, M. Walter, Z. Zeng and K. W. Jacobsen, *J. Phys.: Condens. Matter*, 2017, **29**, 273002.

2 M. Chigaev, J. S. Smith, S. Anaya, B. Nebgen, M. Bettencourt, K. Barros and N. Lubbers, *The Journal of Chemical Physics*, 2023, **158**, 184108.

3 J. S. Smith, B. Nebgen, N. Lubbers, O. Isayev and A. E. Roitberg, *J. Chem. Phys.*, 2018, **148**, 241733.

4 V. Mironov, Y. Alexeev, V. K. Mulligan and D. G. Fedorov, *Journal of Computational Chemistry*, 2019,

40, 297–309.

5 X. Gao, F. Ramezanghorbani, O. Isayev, J. S. Smith and A. E. Roitberg, *J. Chem. Inf. Model.*, 2020, **60**, 3408–3415.

6 S. Boothroyd, P. K. Behara, O. C. Madin, D. F. Hahn, H. Jang, V. Gapsys, J. R. Wagner, J. T. Horton, D. L. Dotson, M. W. Thompson, J. Maat, T. Gokey, L.-P. Wang, D. J. Cole, M. K. Gilson, J. D. Chodera, C. I. Bayly, M. R. Shirts and D. L. Mobley, *J. Chem. Theory Comput.*, 2023, **19**, 3251–3275.

7 L. Wang, P. K. Behara, M. W. Thompson, T. Gokey, Y. Wang, J. R. Wagner, D. J. Cole, M. K. Gilson, M. R. Shirts and D. L. Mobley, *J. Phys. Chem. B*, 2024, **128**, 7043–7067.

8 R. Salomon-Ferrer, D. A. Case and R. C. Walker, *WIREs Computational Molecular Science*, 2013, **3**, 198–210.

9 J. Wang, R. M. Wolf, J. W. Caldwell, P. A. Kollman and D. A. Case, *Journal of Computational Chemistry*, 2004, **25**, 1157–1174.

10 Gaussian 09, Revision E.01, M. J. Frisch, G. W. Trucks, H. B. Schlegel, G. E. Scuseria, M. A. Robb, J. R. Cheeseman, G. Scalmani, V. Barone, G. A. Petersson, H. Nakatsuji, X. Li, M. Caricato, A. Marenich, J. Bloino, B. G. Janesko, R. Gomperts, B. Mennucci, H. P. Hratchian, J. V. Ortiz, A. F. Izmaylov, J. L. Sonnenberg, D. Williams-Young, F. Ding, F. Lipparini, F. Egidi, J. Goings, B. Peng, A. Petrone, T. Henderson, D. Ranasinghe, V. G. Zakrzewski, J. Gao, N. Rega, G. Zheng, W. Liang, M. Hada, M. Ehara, K. Toyota, R. Fukuda, J. Hasegawa, M. Ishida, T. Nakajima, Y. Honda, O. Kitao, H. Nakai, T. Vreven, K. Throssell, J. A. Montgomery, Jr., J. E. Peralta, F. Ogliaro, M. Bearpark, J. J. Heyd, E. Brothers, K. N. Kudin, V. N. Staroverov, T. Keith, R. Kobayashi, J. Normand, K. Raghavachari, A. Rendell, J. C. Burant, S. S. Iyengar, J. Tomasi, M. Cossi, J. M. Millam, M. Klene, C. Adamo, R. Cammi, J. W. Ochterski, R. L. Martin, K. Morokuma, O. Farkas, J. B. Foresman, and D. J. Fox, Gaussian, Inc., Wallingford CT, 2016.

11 R. Ditchfield, W. J. Hehre and J. A. Pople, *J. Chem. Phys.*, 1971, **54**, 724–728.

12 J.-D. Chai and M. Head-Gordon, *The Journal of Chemical Physics*, 2008, **128**, 084106.

13 P. Eastman, J. Swails, J. D. Chodera, R. T. McGibbon, Y. Zhao, K. A. Beauchamp, L.-P. Wang, A. C. Simmonett, M. P. Harrigan, C. D. Stern, R. P. Wiewiora, B. R. Brooks and V. S. Pande, *PLOS Computational Biology*, 2017, **13**, e1005659.

14 D. L. Mobley, C. C. Bannan, A. Rizzi, C. I. Bayly, J. D. Chodera, V. T. Lim, N. M. Lim, K. A. Beauchamp, D. R. Slochower, M. R. Shirts, M. K. Gilson and P. K. Eastman, *J. Chem. Theory Comput.*, 2018, **14**, 6076–6092.